EasyChair Preprint

№ 14856

Managing Epidemics: Dynamic Countermeasures and Frictions

Felix Zurek, Leander Schwarzmeier, Benedetta Dionisi Ferrera, Christina Kuttler and Joachim Draeger

September 13, 2024

Managing Epidemics: Dynamic Countermeasures and Frictions

Felix Zurek, Leander Schwarzmeier, Benedetta Dionisi Ferrera, Christina Kuttler[1], and Joachim Draeger[2]

[1] Technical University of Munich, Department of Mathematics
kuttler@ma.tum.de
[2] IABG mbH, Ottobrunn
draeger@iabg.de

Abstract

After an epidemic outbreak, government and medical institutions try to mitigate the consequences with suitable interventions. Unfortunately, interventions that seem to be successful in theory may be degraded in practice by manifold types of frictions such as delays and erroneous situation assessments. This paper discusses the effects of such frictions. For this purpose, a traditional compartmental model is supplemented by a rule-based control unit, which sets countermeasures into effect when situation assessments exceed critical threshold values.

The model, based on a classical compartmental model, is used to represent the chain of events which occurred in Italy in early 2020. Using analytical considerations, we focus on stability and on the calculation of the reproduction number. With the help of simulation runs, we also investigate the sensitivity of the model parameters and the potential influence of the control unit. The paper concludes with a discussion of the limitations of the underlying model and of the executed analysis.

1 Introduction

In a prophetic Ted talk in 2015, Bill Gates warned about the dangers of a pandemic [16], followed by a more detailed elaboration [17] of his viewpoint in course of the COVID-19 pandemic. Though COVID-19 seems to be almost harmless compared to e.g. infamous Ebola, [33] states 6,952,509 deaths worldwide caused by this virus until July 26th, 2023. This makes COVID-19 one of the most deadliest pandemics in history.

Naturally, there is a strong interest in mitigating such an outbreak. Computer simulations of models representing both, epidemics and various interventions, are often used for that purpose. Depending on the specific illness and the chosen perspective, diverse models have been proposed [21]. Having COVID-19 in mind, we focus on an SEIR model [7], extended by compartments for hospitalized persons, persons being in a critical medical condition, and dead individuals. Without being too detailed, this extension makes the model more suitable for assessing the effectiveness of specific countermeasures. A control unit evaluates the outbreak situation continuously by using a score function. Based on this situation assessment, the control unit decides about actions to be taken in course of intervention management. In the model, these actions are represented by an adaption of model parameters like the infection rate β. The decisions are made based on comparisons between the score function and predefined thresholds. After making the decision, the chosen actions are executed. We distinguish between decision and execution, because frictions may lead to an imperfect implementation of the chosen decision. Frictions have typically the tendency to worsen the situation [4]. Though one is naturally interested in avoiding any friction, they are more or less inevitable e.g. due to the time required

for making a decision. The extension of a traditional epidemic model by a control unit and by frictions aims at the provision of a more comprehensive model of intervention management. Such a model may help to identify better suitable criteria for starting (and maybe ending) interventions. Though the motivation for our work lies in the realm of the COVID-19 pandemic, the authors intend to provide a more general insight into the mechanisms and possible obstacles to control an epidemic.

The paper is organized as follows. After an overview of related work in section 2, we introduce the proposed model in section 3. Section 4 shows how the model is calibrated for representing the chain of events in Italy in early 2020. The model is analyzed using theoretical methods in section 5. Afterwards, Section 6 investigates the model based on simulation experiments. Limitations of the underlying model and of the executed analysis are addressed in section 7. The paper closes with a discussion and an outlook in section 8.

2 Related Work

COVID-19 has shown that the capability of predicting the evolution of an epidemic is of vital interest. But it has also led to the insight that considerations restricted to the epidemics domain will not necessarily give a realistic picture [22]. The inclusion of economics [30, 13], for example, is mandatory for assessing the consequences of interventions from a global perspective, because trying to fight an epidemic usually impairs economics. Another domain influencing the evolution of an epidemic by affecting the effectiveness of interventions is psychology [35, 19]. Being in a potentially dangerous situation of course changes the behavior of the population [20]. The influence of rumors on the compliance with countermeasure regulations has been analyzed in [15] and, more detailed, in [14]. Rumors are an example, how misinformation may influence human behavior [18]. A general model of cognitive information processing and thus on the influence of human biases and of irrationality on decision-making is developed in [11]. The paper [11] focuses on social engineering as exemplary application instead of epidemics, though. It follows the basics of risk assessment, i.e. analyzing the effects of an off-nominal (i.e. irrational in our case) behavior of the underlying system (see e.g. [10, 12]).

The design of control strategies for intervention planning during disease outbreaks is the topic of [26, 36, 37]. A corresponding holistic systems informatics approach is discussed in [42]. Specific intervention strategies are analyzed in [9]. The paper [25] describes a framework for analyzing suitable strategies for disease containment. It takes limited resources into account as well. A decision support system aiming in the protection of critical infrastructures in case of an outbreak is presented in [24]. The topic of response planning is also addressed in [29]. A multi-domain analysis of the intervention problem is given in [22]; here, Larson and Nigmatulina state that despite of all medical interventions, the control of epidemics via social contact rate may be the most effective countermeasure. An epidemics control with inclusion of organizational delays is discussed in [38].

3 Model Description

The paper investigates suitable intervention strategies, when interventions are only applied when a continuously worsening situation triggers corresponding actions and when interventions are affected by frictions. This leads to a heterogeneous modeling approach, in which an ODE describing the evolution of the epidemics is supplemented by a rule system representing a control unit. The control unit tries to mitigate the consequences of the epidemic by setting counter-

measures into effect. In our case, these interventions are represented by changing the values of some model parameters correspondingly. Non-idealism is taken into account by the possibility of an erroneous number of infectious persons and by the inclusion of delayed interventions due to non-instantaneous decision processes, communication needing some time, and bureaucratic processes.

3.1 ODE Model

We model epidemics by extending the standard SEIR model [27]. Such an model is a quite prominent tool for describing outbreaks of COVID-19 [7] and other diseases with a relevant incubation period. We extend the standard SEIR model with compartments of hospitalized H, critical C and dead D individuals analogous to [39]. This gives the epidemics model shown in figure 1).

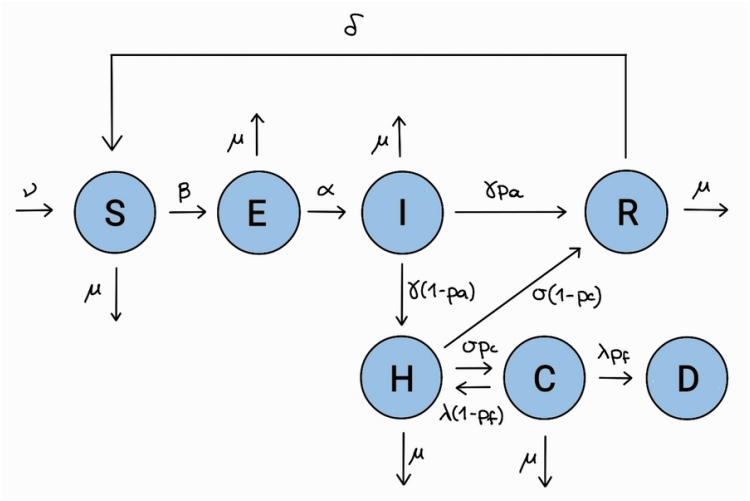

Compartments	
S	Susceptibles
E	Exposed
I	Infected
H	Hospitalized
C	Critical (ICU)
R	Recovered
D	Dead

Figure 1: Flowchart of the SEIHCRD Model (1) (left); list of model compartments (right)

In the model, susceptible individuals can get infected when in contact with an infectious individual. This is represented in the model by a flow from the compartment S of susceptibles to the compartment E of so-called exposed individuals. Exposed individuals are infected, but not yet infectious. Becoming infectious after some time is represented by a flow from E to the compartment I of infected individuals with a rate α. Infectious individuals can either recover by transition to the compartment R, or have to be hospitalized due to a worsening condition. The latter case is described by a flow to the compartment H. Hospitalized individuals can recover as well or have to be transferred to intensive care units, which are represented by the compartment C. Patients who could be stabilized move back to the state 'hospitalized'. Otherwise they die and end up in the compartment D, which only tracks disease related deaths. Additionally, we introduce vital dynamics by a birth rate ν increasing S and a natural death rate μ not related to COVID-19, affecting all compartments except D. This gives the following ordinary differential

equation system:

$$\begin{aligned} S'(t) &= -\beta I(t)S(t)N^{-1} + \delta R(t) + \nu - \mu S(t) \\ E'(t) &= \beta S(t)I(t)N^{-1} - \alpha E(t) - \mu E(t) \\ I'(t) &= \alpha E(t) - \gamma I(t) - \mu I(t) \\ H'(t) &= \gamma(1-p_a)I(t) + \lambda(1-p_f)C(t) - \sigma H(t) - \mu H(t) \\ C'(t) &= \sigma p_c H(t) - \lambda C(t) - \mu C(t) \\ R'(t) &= \gamma p_a I(t) + \sigma(1-p_c)H(t) - \delta R(t) - \mu R(t) \\ D'(t) &= \lambda p_f C(t) \end{aligned} \tag{1}$$

with $N = S + E + I + H + C + R$. The meaning of the parameters of the ODE system (1) is described in Table 1.

Parameters	Meaning
$\alpha \in \mathbb{R}^+$	Rate of being infected
$\beta \in \mathbb{R}^+$	Transmission rate
$\gamma \in \mathbb{R}^+$	Rate of leaving the state 'infectious'
$\delta \in \mathbb{R}^+$	Rate of becoming susceptible again after recovery
$\sigma \in \mathbb{R}^+$	Rate of leaving the state 'hospitalized' (either by recovery or transfer to the ICU)
$\lambda \in \mathbb{R}^+$	Rate of leaving the state 'being in critical condition' (either by becoming hospitalized again or by dying)
$p_a \in [0,1]$	Fraction of infected individuals needing no hospital treatment
$p_c \in [0,1]$	Fraction of hospitalized agents switching to a critical state
$p_f \in [0,1]$	Fraction of critical cases resulting in death
$\nu \in \mathbb{R}^+$	Birth rate
$\mu \in \mathbb{R}^+$	Natural death rate

Table 1: Parameters of model (1)

The parameters $\alpha, \beta, \gamma, \delta, \sigma, \lambda, \nu$ and μ have the unit days^{-1}. The parameters p_a, p_c and p_f are unit-less, as denoting fractions. We have introduced vital dynamics, i.e. births and natural deaths, since a stability analysis without vital dynamics is inadequate. Usually, vital dynamics does not influence the outcome of a single epidemic outbreak too much due to the different time scales of both processes.

3.2 Control Unit and Frictions

In the following, only countermeasures that can be represented by a reduction in the infection rate β are considered like for example wearing a mask or social distancing. For this purpose the value of β is multiplied by a corresponding scaling factor [8]. This approach is capable of including the unwillingness of parts of the population to follow the regulations as well by modifying the scaling factor. Countermeasures are set into effect by the control unit.

Including an explicit control is not very common. Up to the knowledge of the authors, corresponding discussions do not exist in the literature up to now. Usually, it is assumed that the countermeasures are setting in at a given time. A simple version of such a control process can be represented by a set of condition-action rules. The condition part of a rule will be triggered by a situation assessment measure exceeding a critical threshold. As a consequence, the related intervention action will be executed. As indicated above, this means a corresponding reduction of β.

For improving the faithfulness of the model, imperfections — hereafter also called frictions — both in the application of the countermeasures and in the decision-making process are taken into account. In order to keep the upcoming analysis at a simple level, we include only two different kinds of frictions:

Imperfect observations: Imperfect observations refer to the existence of measurement errors. We specifically consider a difference between observed and actual infections. Such a difference can be attributed to various factors, such as limited testing capacity or asymptomatic cases going undetected [34]. Delays in case reporting may contribute to this effect as well. Imperfect observation can lead to a dangerous underestimation of the epidemic [40].

Delay in actions: Delays may occur in all steps of the decision-making process. It may take some time to recognize the need for an intervention, to actually make a decision and to implement the specific countermeasures decided upon. Naturally, delays can impact the timeliness of interventions.

Definition (Control Unit) The control unit decides about required actions based on the current state $x(t) = (S(t), E(t), I(t), H(t), C(t), R(t), D(t))^T$. The decision process is parameterized by:

1. Compartment weights $w_I, w_H, w_C, w_D \in \mathbb{R}^+$
2. (Mean) Observation correctness $\varepsilon \in [0, 1]$
3. Action thresholds T_1, T_2, $T_3 \in [0, 1]$ with $T_1 < T_2 < T_3$
4. Effectiveness η_1, η_2, $\eta_3 \in [0, 1]$ of countermeasures
5. (Mean) Delay $\tau \in \mathbb{R}^+$

The number of actually infected people is given by I whereas εI is the number of detected cases. The compartment weights are used in the *score function*

$$\Phi(x(t), w_I, w_H, w_C, w_D, \varepsilon) = \frac{w_I \varepsilon I(t) + w_H H(t) + w_C C(t) + w_D D(t)}{w_I + w_H + w_C + w_D} \tag{2}$$

for assessing the criticality of the current system state $x(t)$. If the score function value exceeds a given threshold T_i, the control unit sets corresponding countermeasures into effect. This is represented by a reduction in the transmission rate β by scaling β with the corresponding efficiency η_i. This reduction takes place with a delay τ after T_i has been triggered. From then on, the ODE system (1) is solved with $\beta' = \eta_i \beta$ instead of β. For reasons of simplicity, we only consider the activation of countermeasures, but not their de-activation.

The compartment weights determine the individual importance of the corresponding compartment levels in the criticality assessment. We use the exemplary values given in Table 2. They have been chosen just based on an educated guess. A large number of fatalities is undoubtedly most alarming, hence it has the highest weight. The number of infected individuals is associated with the second highest weight. Though the number of e.g. persons in intensive

care seems to be more alarming, it allows a much more instantaneous reaction contrary to hospitalized persons or persons in critical care in case of COVID-19 [21] due to the usually large time gap between infection and requiring an ICU. Finally, we use a weight w_C larger than w_H in order to highlight intensive care unit (ICU) beds and caring personnel as a more valuable and limited resource than standard hospital beds.

Compartments	Weights
D	$w_D = 0.5$
I	$w_I = 0.25$
C	$w_C = 0.15$
H	$w_H = 0.1$

Table 2: Values of the compartment weights

Many countries tracked the number of infected, hospitalized, critical and dead individuals and based their intervention management on these data [3]. Different lockdown levels with different rules and varying degrees of effectiveness have been introduced depending on whether certain thresholds are reached [2]. This relates to the structure of the control unit in the definition. With a balance of complexity and faithfulness in mind, three different thresholds T_i with associated effectivenesses η_i are distinguished.

3.3 Model Behavior

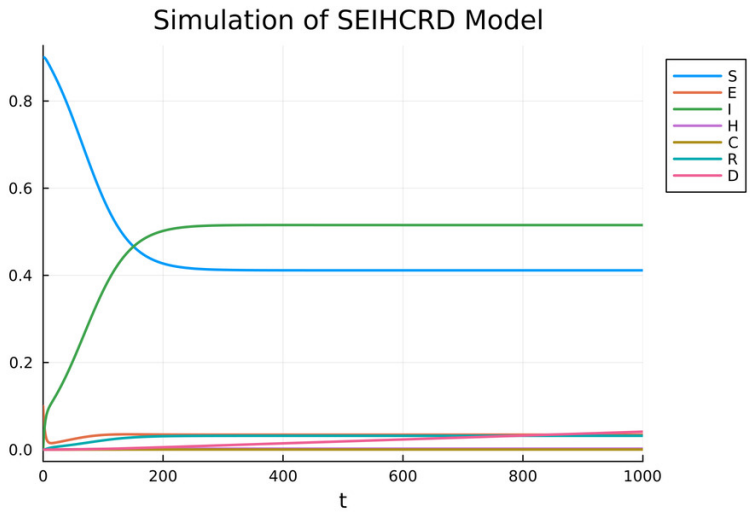

$\alpha = 0.3$	$\gamma = 0.01$	$\sigma = 0.5$	$p_a = 0.79$	$p_f = 0.33$	$\nu = 0.01$
$\beta = 0.05$	$\delta = 0.15$	$\lambda = 0.5$	$p_c = 0.12$		$\mu = 0.01$

Figure 2: Dynamics of the model without control unit

The proposed model was implemented in the Julia programming language [5], whereby the differential equations package and its solvers has been used [31]. Utilizing so-called callback functions [1], we can access and change the parameters of the differential equation system during the numerical integration. This allows a straightforward implementation. We will now

showcase a few examples. Figure 2 shows a situation in which the levels of the compartments S, E, I, H, C, R converge to a non-zero equilibrium, whereas the level of deaths D steadily increases. Due to the non-zero equilibrium of I and S, the flow to the compartment D is compensated by the birth rate. In case of a larger value of γ, the epidemic dies out.

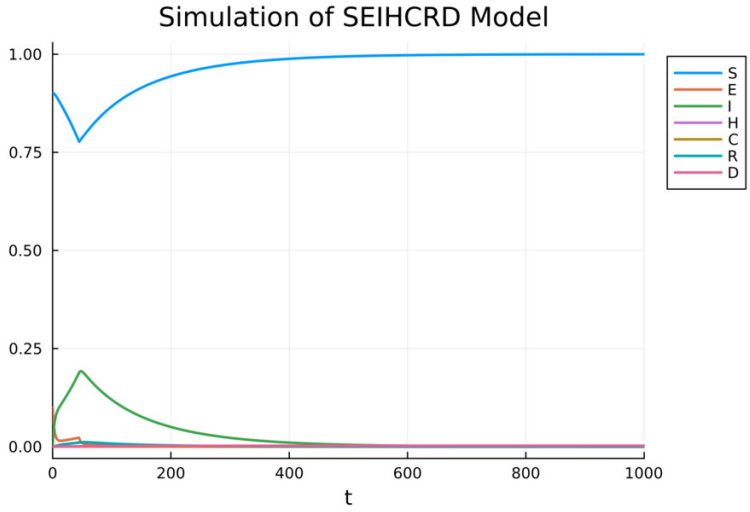

$\alpha = 0.3$	$\gamma = 0.01$	$\sigma = 0.5$	$p_a = 0.79$	$p_f = 0.33$	$\nu = 0.01$
$\beta = 0.05$	$\delta = 0.15$	$\lambda = 0.5$	$p_c = 0.12$		$\mu = 0.01$

$(w_I, w_H, w_C, w_R) = (0.25, 0.1, 0.15, 0.5)$	$(T_1, T_2, T_3) = (0.04, 0.05, 0.1)$
$\tau = 10$, $\varepsilon = 1$	$(\eta_1, \eta_2, \eta_3) = (0.25, 0.5, 0)$

Figure 3: The inclusion of a control component changes the dynamics fundamentally compared to Figure 2 despite of unchanged parameter values.

We will now apply interventions. In the situation of figure 3 with a delay of $\tau = 10$ days, countermeasures are implemented after roughly 45 days leading to an extinction of the disease and to a total number of deaths of only 0.0025. When a shorter delay of only 1 day is used, the control unit would intervene after 35 days leading again to the extinction of the disease and to a number of deaths of now 0.002. When the delay in increased to the very large value of $\tau = 100$ days, the control unit steps in three times: after 135, 148, and 211 days. The epidemic still dies out, resulting in a death rate of 0.0056. Coming back to the example of figure 3 with $\tau = 10$ days, we will now increase the number of unregistered cases by reducing ε to $\varepsilon = 0.6$. In this case, an intervention is realized after 78 days. The number of dead individuals would rise to 0.04 compared to 0.0025 for $\varepsilon = 1.0$.

The results can be summarized in such a way that the presence of a control unit can lead to fundamental changes. Triggering suitable countermeasures may lead to an effective decrease of infection numbers and thus to a successful epidemics management. Naturally, frictions can be disadvantageous. They may postpone or scale down the effects of interventions.

4 Application to COVID-19

We will now apply the model to the case of COVID-19 for validating our modeling approach. This may also be a good opportunity to gain new insights into intervention management. We

use the data set [28], which compiles the official numbers of infections, hospitalizations, ICU-patients and deaths for many countries. The numerical calculations are done using R.

We focus on the pandemic at a country level, because observation processes and intervention management are executed more or less consistently. In this respect, e.g. Germany was excluded as a candidate for a deeper analysis due to its federal structure and the associated in-homogeneous countermeasure management. Italy is considered as being much more suitable, because the chosen counter-measures are well documented and the case numbers have been updated daily. We will look at the time frame before and after the first lockdown, i.e. at the time interval between 22/02/2020 (first case numbers are reported) and 15/05/2020 (the lockdown was eased). Due to the short period of time, the model parameters are assumed to be constant; it is not necessary to take virus mutations with different illness characteristics into account [41].

Some of the model parameters result from illness data in a straightforward manner. This especially concerns the values of α and γ, which are determined by the mean incubation period and the mean duration of infectiousness. We get $\alpha = 1/5.2 = 0.192$ [23]. For the parameter γ, the value $\gamma = 1/7 = 0.143$ is chosen [6] a bit arbitrarily; in literature, many different values are proposed. Due to short time interval under consideration, we set $\delta = 0$.

Using these values of α, γ and δ, we now fit the SEIR submodel to the available observation data. We ignore the compartments H, C and D at first, since their influence on the overall dynamics of the COVID-19 epidemic is quite limited. We use the total numbers for the compartment levels with $N = 6 \cdot 10^7$ for Italy. With regard to the parameters of the SEIR submodel, it remains to determine β. During the time interval of interest a lockdown have become effective, but ahead of the lockdown the evolution of the epidemics is indeed guided by the original β. We therefore choose a cut-off date t' for the trajectories and select the value of β in such a way that the mean square error between the simulation trajectory $I(t)$ and the corresponding real data is minimized. After doing so for multiple cutoff dates t', we take the date t' together with the associated β value that best fits the data. This gives $t' = 18/03/2020$ and $\beta = 0.555$. For $t \geq t'$, we get a best fit for $\beta = 0.094$ (see figure 4).

Note that no real-world data are available for E. The plot contains a second order discontinuity when the lockdown takes effect. The level of E decreases immediately after the discontinuity, while I still increases for some more days. The date $t' = 18/03/2020$ is an interesting finding by itself. On the 9th of March 2020, Italy extended the lockdown, which up to this time has been raised only to some special areas, to a nation-wide lockdown. As the lockdown takes effect on March the 18th, this gives a delay of 9 days between decision and effective execution. This validates the proposed delay of ten days. Concerning the reproduction number $R_0 = \beta/\gamma$, the outbreak starts with $R_0 = 3.88$. When the lockdown is set into effect, the corresponding value is $R_0 = 0.66 < 1$ and so the epidemic vanishes. This gives a reduction of β by a scaling factor equal to 0.17.

What remains to be done is to fit $\sigma, \lambda, p_a, p_c, p_f$. Remarkably, the predicted number of hospitalizations seems to exceed the real-world case numbers by far (see Figure 5). One would expect that hospitalized people are included in the number of infected persons and thus $I(t) \geq H(t)$. Furthermore, the disease was not that severe that a large part of the infected persons needed to be hospitalized. However, it should be noted that Italy gives the number of patients in hospitals as a cumulative number, whereas the number of infections counts the *new* infections on a daily base. Beyond that, due to the insufficient availability of test kits in early 2020 — there were no rapid antigen tests at all — many new infections remained undetected. Hospital patients, in the contrary, were recorded in full without any unreported cases.

Overall, the model describes the dynamics of the COVID-19 pandemic quite well. The decrease in β resulting from the countermeasures is appropriately represented as well. Accord-

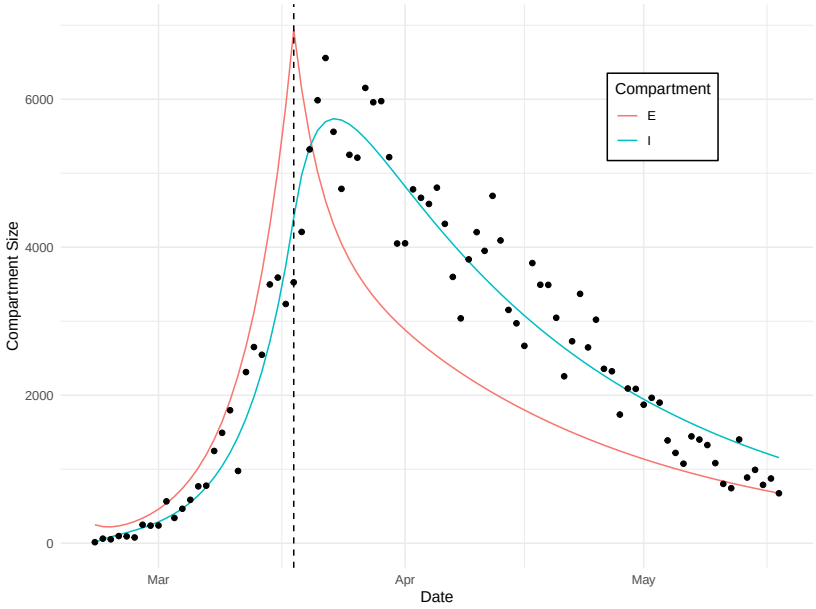

Figure 4: $\beta = 0.555$ before, $\beta = 0.094$ after the lockdown.

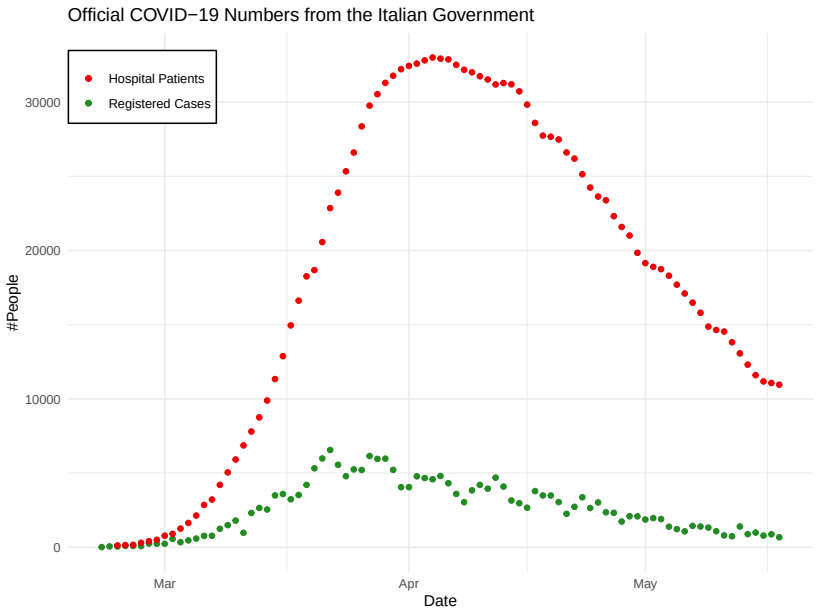

Figure 5: The number of hospitalizations is way higher than the amount of registered cases

ingly, we consider the proposed model as being essentially valid though it was not possible to validate the part of the model dealing with H, C and D at an appropriate level.

5 Theoretical Analysis

In this section we collect some basic analytical results.

5.1 Stability Analysis

Let us start analyzing stability of the ODE model (1). We will neglect the model extensions consisting of control unit and frictions. For this purpose, we will take a closer look at the equilibrium points of model (1) and at the behaviour of the model in the proximity to these equilibria. Following [27], we focus on disease-free equilibria, linearize the defining equations and check the sign of the eigenvalues' real parts.

Due to the structure of the set of equilibrium points $\widetilde{P}$, it is not necessary to take the equation for compartment D into account. In order to determine the stationary points, every equation of system (1) is set equal to zero. This gives the equation system

$$\begin{array}{ll} -\beta I(t)S(t)/N + \delta R(t) + \nu - \mu S(t) & = 0 \\ \beta S(t)I(t)/N - (\alpha+\mu)E(t) & = 0 \\ \alpha E(t) - (\gamma+\mu)I(t) & = 0 \\ \gamma(1-p_a)I(t) + \lambda(1-p_f)C(t) - (\sigma+\mu)H(t) & = 0 \\ \sigma p_c H(t) - (\lambda+\mu)C(t) & = 0 \\ \gamma p_a I(t) + \sigma(1-p_c)H(t) - (\delta+\mu)R(t) & = 0 \end{array} \tag{3}$$

From the third and the fifth equation in the system shown above, we get

$$E^* = \frac{\gamma+\mu}{\alpha} I^* \quad \text{and} \quad H^* = \frac{\lambda+\mu}{\sigma p_c} C^*.$$

Substituting H^* in the fourth equation and E^* in the second one leads to

$$\begin{array}{rcl} C^* & = & -\frac{\gamma\sigma p_c(1-p_a)}{\lambda\sigma p_c(1-p_f)-(\sigma+\mu)(\lambda+\mu)} I^* \\ \implies H^* & = & -\frac{\gamma(1-p_a)(\lambda+\mu)}{\lambda\sigma p_c(1-p_f)-(\sigma+\mu)(\lambda+\mu)} I^* \end{array}$$

and to

$$I^* \left(\tfrac{\beta S^*}{N} - \tfrac{(\alpha+\mu)(\gamma+\mu)}{\alpha} \right) = 0 \iff I^* = 0 \vee S^* = \tfrac{(\alpha+\mu)N}{\alpha\beta}.$$

This yields two potential equilibria.

Case $I^* = 0$: Due to the case assumption, the last equation of (3) immediately gives $R^* = 0$. Substituting $I^* = 0$ and $R^* = 0$ in the first equation of (3) yields $\nu - \mu S^* = 0 \iff S^* = \nu/\mu$. We get $\widetilde{P} = (\nu/\mu, 0, 0, 0, 0, 0)$ as the disease-free equilibrium.

Case $S^* = \dfrac{(\alpha+\mu)N}{\alpha\beta}$: Substituting the case assumption in the first equation of (3) gives.

$$R^* = \frac{(\alpha+\mu)(\gamma+\mu)}{\alpha\delta} \left(I^* + \frac{N}{\beta} \right) - \frac{\nu}{\delta}.$$

Using this intermediate result, the last equation of (3) can be rewritten as

$$I^* = \left(-\frac{\sigma\gamma(1-p_c)(\lambda+\mu)(1-p_a)}{\lambda(1-p_f)+(\sigma+\mu)(\lambda+\mu)} + \frac{\alpha\beta\gamma\delta p_a - (\delta+\mu)(\alpha+\mu)(\gamma+\mu)}{\alpha\beta\delta} \right)^{-1} \cdot \left(\frac{\nu\alpha\delta + (\delta+\mu)(\alpha+\mu)(\gamma+\mu)}{\alpha\delta} \right).$$

Defining $\widetilde{E}, \widetilde{H}, \widetilde{C}, \widetilde{R}$ as results of inserting I^* in the expressions of E^*, H^*, C^*, R^* gives

$$\widetilde{P}' = \left(\frac{(\alpha+\mu)N}{\alpha\beta}, \widetilde{E}, I^*, \widetilde{H}, \widetilde{C}, \widetilde{R} \right),$$

as non-disease-free equilibrium.

We focus now on the disease-free equilibrium $\widetilde{P}$. The system (1) is linearized using the Jacobian matrix $J(\widetilde{P}) \in M_{\mathbb{R}}(6,6)$. We obtain $\dot{X} = JX$ with $X := (S, E, I, H, C, R)$. The eigenvalues of J at the point $\widetilde{P}$ — in the following referred to as $\widetilde{J}$ — can be determined using the characteristic polynomial

$$p_{\widetilde{J}}(\ell) = det(\widetilde{J} - \ell I) = (\ell+\mu)(\ell+\delta+\mu)p_1 p_2 \tag{4}$$

with

$$\begin{aligned} p_1 &= (\ell+\alpha+\mu)(\ell+\gamma+\mu) - \alpha\beta \\ &= \ell^2 + \ell(\gamma+2\mu+\alpha) + (\mu^2+\mu\gamma+\mu\alpha+\alpha\gamma-\alpha\beta) \\ p_2 &= (\ell+\mu+\lambda)(\ell+\mu+\sigma) - \sigma p_c\lambda(1-p_f) \\ &= \ell^2 + \ell(\sigma+2\mu+\lambda) + (\mu^2+\mu\sigma+\mu\lambda+\lambda\sigma-\sigma\lambda p_c(1-p_f)) \end{aligned} \tag{5}$$

We obtain

$$\begin{aligned} \ell_1 &= -\mu \\ \ell_2 &= -(\delta+\mu) \end{aligned}$$

as roots of the characteristic polynomial (4). Regarding the roots of p_1 and p_2, we get respectively:

$$\begin{aligned} \ell_{3,4} &= \frac{1}{2}\left(-(\alpha+2\mu+\gamma) \pm \sqrt{(\alpha+2\mu+\gamma)^2 - 4(\mu^2+\mu\gamma+\mu\alpha+\alpha\gamma-\alpha\beta)} \right) \\ \ell_{5,6} &= \frac{1}{2}\left(-(\lambda+2\mu+\sigma) \pm \sqrt{(\lambda+2\mu+\sigma)^2 - 4(\mu^2+\mu\sigma+\mu\lambda+\lambda\sigma-\sigma\lambda p_c(1-p_f))} \right). \end{aligned}$$

We already know that $\ell_1, \ell_2, \ell_4, \ell_6, \ell_7$ are negative and that it holds

$$\ell_3 < 0 \iff \beta < \frac{\mu^2+\mu\gamma+\mu\alpha+\alpha\gamma}{\alpha}. \tag{6}$$

We can state that in system (1) the existence of an eigenvalue $\ell = 0$ can be avoided. A more detailed analysis [43] shows that this is realized by the exclusion of the equation related to the compartment D. Note that an eigenvalue $\ell = 0$ would prevent the application of the Hartman-Grobman theorem, which requires non-zero real parts as a prerequisite for all eigenvalues. However, it is precisely this theorem that enables us to derive the qualitative behaviour of the non-linear system from that of the linearised system. We can state that the stability conditions will change at the critical value $\beta = (\mu^2+\mu\gamma+\mu\alpha+\alpha\gamma)/\alpha$. The equilibrium is stable iff (6) holds.

5.2 Reproduction Number

The so-called reproduction number R_0 [27] gives the average number of new infections in a fully susceptible population caused by a single infected person. For determining R_0, we will follow the next-generation approach. The idea is to define the so-called next-generation matrix, which relates the number of infected individuals in the different compartments in consecutive generations. Then, the reproduction number R_0 is given by the spectral radius of the next-generation matrix.

We study the differential equation system (1) with compartment D being excluded. We define X as the vector of variables in the infected compartments and Y as the vector of variables in the non-infected compartments. It holds

$$\begin{aligned} X &= (E, I) \\ Y &= (S, H, C, R). \end{aligned} \tag{7}$$

and so

$$\begin{aligned} \dot{X} &= (\dot{E}, \dot{I}) \\ \dot{Y} &= (\dot{S}, \dot{H}, \dot{C}, \dot{R}). \end{aligned} \tag{8}$$

According to the method of Van den Driessche and Watmought [27], we split up the right-hand side of the infected compartments as follows:

$$\dot{X} = \begin{pmatrix} \beta SI/N \\ \alpha E \end{pmatrix} - \begin{pmatrix} (\alpha+\mu)E \\ (\gamma+\mu)I \end{pmatrix} = \mathcal{F}(X,Y) - \mathcal{V}(X,Y)$$

with $F_i(X,Y)$ as the rate of new infections in compartment $i \in \{E, I\}$ and $V_i(X,Y)$ as the remaining transitional term. This decomposition satisfies the following properties:

1. $\mathcal{F}(0,Y) = 0$ and $\mathcal{V}(0,Y) = 0$ for $Y \geq 0$
2. $\mathcal{F}(0,Y) \geq 0$ for all $X, Y \geq 0$
3. $\mathcal{V}_i(0,Y) \leq 0$ for all $X_i \leq 0$
4. $\sum_{i \in \{E,I\}} \mathcal{V}_i(0,Y) \geq 0$ for all $X, Y \geq 0$

Now we determine the Jacobian matrices $F = D_X\mathcal{F}(X,Y)$ and $V = D_X\mathcal{V}(X,Y)$ and evaluate them in the disease-free equilibrium $\widetilde{P}$. After substituting the equilibrium $\widetilde{P} = (\nu/\mu, 0, 0, 0, 0, 0)$ in the Jacobian matrix, we obtain

$$F = \begin{pmatrix} 0 & \frac{\beta}{\mu(\gamma+\mu)} \\ \alpha & 0 \end{pmatrix} \quad \text{and} \quad V = \begin{pmatrix} \alpha+\mu & 0 \\ 0 & \gamma+\mu \end{pmatrix}$$

Hence, the linearized system for the infected compartments can be written as $\dot{X} = (F - V)X$. The next-generation matrix is defined as FV^{-1} and thus the reproduction number is equal to $R_0 = \rho(FV^{-1})$ with $\rho(A)$ as the spectral radius of A. Therefore, we obtain

$$FV^{-1} = \begin{pmatrix} 0 & \frac{\beta}{\mu(\gamma+\mu)} \\ \frac{\alpha}{\alpha+\mu} & 0 \end{pmatrix} \implies R_0 = \rho(FV^{-1}) = \sqrt{\frac{\alpha\beta}{(\alpha+\mu)(\gamma+\mu)}}.$$

It holds

$$R_0 < 1 \iff \frac{\alpha\beta}{(\alpha+\mu)(\gamma+\mu)} < 1$$

which is nothing else than condition (6). It shows the dependency of R_0 on the model parameters α, β and γ.

6 Simulation-based Analysis

In the following we show some results determined by extensive simulations of the ODE model.

6.1 General Remarks

The purpose of a sensitivity analysis is to assess the effects of parameter changes on the outcome. Concerning the parameter of a differential equation system like (1), [32] defines the sensitivity of a solution $x(t,p)$ with respect to a parameter p as

$$S_p(t) = \frac{dx(t,p)}{dp} \tag{9}$$

The time derivative of $S_p(t)$ for the i-th equation f_i of system (1) is given by

$$\frac{dS_{ip}}{dt} = \frac{\partial f_i}{\partial p} + \sum_{j=1}^{n} \frac{\partial f_i}{\partial x_j} S_{jp} \tag{10}$$

Since compartmental models of epidemics are well known and already analyzed in depth, we will focus on the sensitivity of the parameters of the control unit (see section 3.2). The approach (10) cannot be applied in a straightforward manner here, though, because the control unit is not defined based on a differential equation system. Thus, the derivative in definition (9) is replaced by a finite difference:

$$S_{ip}(t) = \frac{x_i(t,p+h) - x_i(t,p)}{h} \quad \text{for } i \in \{1,...,7\} \tag{11}$$

6.2 Delay

The sensitivity $S_{i\tau}$ for the delay parameter τ is shown in figure 6. It is the highest for $\tau = 0$ across all compartments and it is almost zero for $\tau > 0$. This means that the system answers quite sensitively on an almost instantaneous reaction, whereas the impact of reactions with some more delay is significantly damped out.

If γ is large enough, the epidemic dies out and the sensitivity concerning delays becomes zero. For very large δ, ν or μ, the sensitivity reaches zero as well. In case of $p_c \geq 0.35$, a strong sensitivity peak related to D appears. The larger the value of p_c, the earlier this peak occurs. For large values of ν, the trajectory of $S_{D\tau}(t)$ may contain a second peak. Concerning variations of η, one, two or three peaks can be seen in $S_{D\tau}(t)$ (see Figure 7). For large η_1, the sensitivity decreases significantly, as at some point no more new infections occur and the number of deaths can therefore no longer increase. The number of peaks relates to the number of activated countermeasures.

Figure 8 demonstrates the effects of a variation of the delay parameter τ between 0 — meaning instant intervention — and 1000 days. For reasons of simplicity, we restrict our considerations to a single control rule. Concerning countermeasure efficiency, $\eta = 0.5$ is assumed.

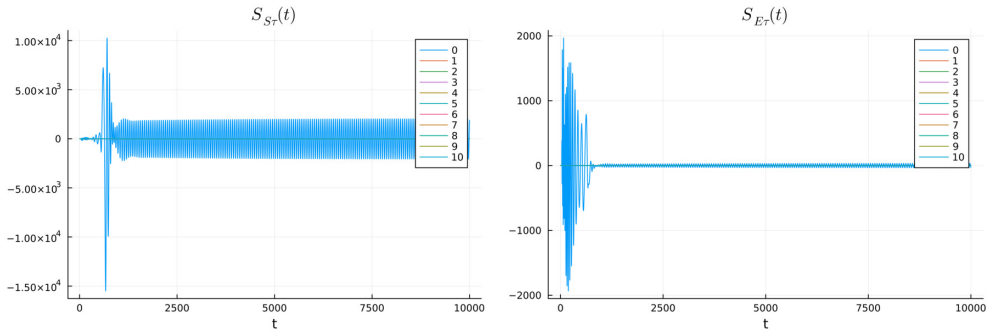

Figure 6: Sensitivities of the delay parameter for S (left) and E (right). The sensitivity of I behaves analogous to $S_{E\tau}$, whereas the sensitivity of H, C, R, and D behaves similar to $S_{S\tau}$

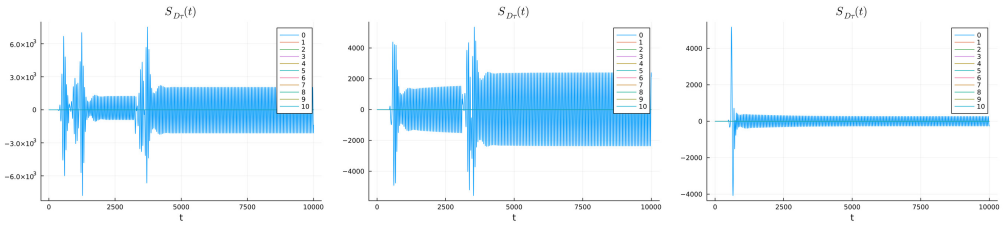

Figure 7: Sensitivity $S_{D\tau}$ for varying η_1

In the general, a large delay can be partially counteracted with choosing a small threshold. In case of a slowly evolving epidemics with long duration, the weights w_I, w_H and w_C have only minor influence on the behaviour of the system. Larger values of the weight w_D optimize the final outcome of the epidemics related to the number of casualties. Concerning observation correctness, we observe a phase transition of the system behavior in the region $\varepsilon \in [0.6, 0.7]$.

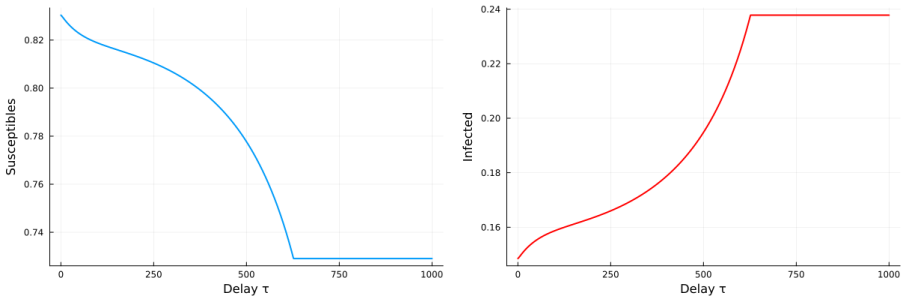

$\alpha = 0.3$	$\gamma = 0.01$	$\sigma = 0.5$	$p_a = 0.12$	$p_f = 0.33$	$\nu = 0.01$
$\beta = 0.05$	$\delta = 0.15$	$\lambda = 0.5$	$p_c = 0.79$		$\mu = 0.01$
$\eta = 0.5$					

Figure 8: Correlations susceptibles-delay and infected-delay respectively.

6.3 Weights of the score function

The compartments E and I typically have significantly lower sensitivities with regard to all four weight parameters than H, C, D, R or S, especially for large t. The sensitivity concerning the weight w_I (see Figure 9) reaches a maximum for $w_I = 0.1$, but it is close to zero for other values of w_I. Often, a small peak for $t \approx 7100$ days can be observed. Variations of the delay τ will typically change the value of w_I with the highest sensitivity. In case of $\tau = 10$, for example, the sensitivity is the highest for $w_I = 0.1$, whereas for $\tau = 20$ the maximum can be found at $w_I = 0.3$.

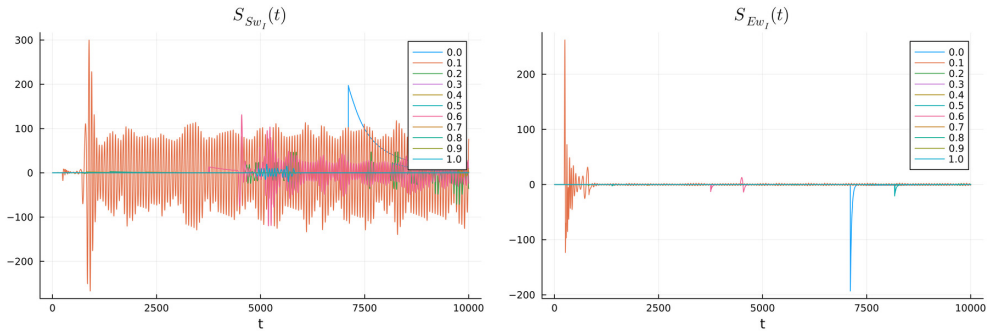

Figure 9: Sensitivity functions S_{Sw_I} (left) and S_{Ew_I} (right). The sensitivity function S_{Iw_I} behaves analogous to S_{Ew_I}.

In general, the sensitivities for w_H are smaller than the ones for w_I but most of the time non-zero. Increasing the delay τ shifts specific sensitivity values to later time points. The sensitivity concerning the parameter w_C is similar to w_H. A larger δ increases the similarity of the sensitivity plots describing the behavior of w_C. For w_D, the sensitivities are larger than for w_C and w_H.

Simulation experiments for a variety of weight values (see Table 3) show that the number of deaths becomes minimal with $(w_I, w_H, w_C, w_D) = (1, 0, 0, 0)$. This result also indicates that an early intervention is crucial: When choosing $(1, 0, 0, 0)$, we focus on I that reaches their maximum earlier than H, C or D. This intervention strategy is very stable under changes of the situation. With larger thresholds T_i, though, weight combinations with non-zero w_D become preferable since the death toll have had time to rise. Concerning the observation correctness ε, an analogous statement can be made.

6.4 Thresholds of the score function

The sensitivity concerning threshold T_1 is shown in figure 10. We observe large values for $(T_1, T_2, T_3) = (0, 0.1, 1)$ and for $(T_1, T_2, T_3) = (0, 0.9, 1)$. For larger values of β, p_c and w_I, the sensitivity becomes large for $(T_1, T_2, T_3) = (0, 0.2, 1)$. For large μ, additional threshold combinations show high sensitivity value.

Variations of T_2 or of T_3 are typically associated with sensitivities close to zero. This means that additional countermeasures beyond the initial intervention usually do not change the system behavior significantly. Concerning a minimization of the death toll, settings like $T_1 = 0, T_2 = 0.01, T_3 = 0.02$ give typically near-optimal results because of an almost immediate intervention.

w_I	w_H	w_C	w_D	D
1	0	0	0	0.000600927689137684
0.9	0.1	0	0	0.000606317131184192
0.9	0	0.1	0	0.0006063397418061638
0.9	0	0	0.1	0.000606368228860041
0.8	0.2	0	0	0.0006173509135282914
0.8	0.1	0.1	0	0.0006174155309946262
0.8	0	0	0.2	0.0006174250868030513
0.8	0.1	0	0.1	0.0006174262724826221
...				
0	0.2	0.8	0	0.4430133790669686
0	0.1	0.9	0	0.4430133790669686
0	0	1	0	0.4430133790669686

$\alpha = 0.3$	$\gamma = 0.01$	$\sigma = 0.5$	$p_a = 0.79$	$p_f = 0.33$	$\nu = 0.01$
$\beta = 0.05$	$\delta = 0.15$	$\lambda = 0.5$	$p_c = 0.12$		$\mu = 0.01$

(w_I, w_H, w_C, w_R) as above	$(T_1, T_2, T_3) = (0.01, 0.05, 0.1)$
$\tau = 0$, $\varepsilon = 0.8$	$(\eta_1, \eta_2, \eta_3) = (0.5, 0.25, 0)$

Table 3: Combination of weights (w_I, w_H, w_C, w_D) and resulting number of deaths in a simulation after $t = 10000$ with the given parameters

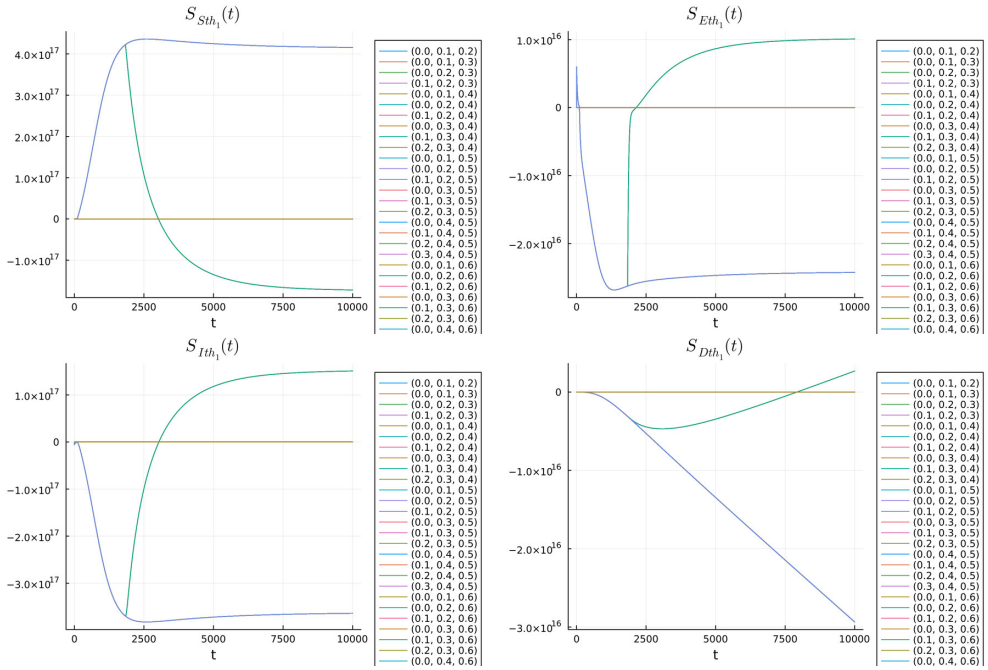

Figure 10: Sensitivity function S_{ST_1}, S_{ET_1}, S_{IT_1}, S_{DT_1}. For the parameter T_1, the sensitivity functions S_{HT_1}, S_{CT_1} and S_{RT_1} show a behaviour very similar to S_{IT_1}.

6.5 Effectiveness of the lockdown

For $\eta_1 = 0$ (complete lockdown), the compartments S, H, C, R, D react highly sensitive. $S_{E\eta_1}$ and $S_{I\eta_1}$ have small values, except for some peaks. This indicates that the system's behaviour changes fundamentally at $\eta_1 = 0$. Higher thresholds result in higher peaks, because in this way an intervention is done only at later times, at which the epidemic is already more advanced.

For η_2, the sensitivity behavior depends on the value of η_1. If the first intervention is already reducing the number of infections significantly, the second countermeasure may not even be triggered at all. For e.g. $\eta_1 = 0.8$, we can observe a high sensitivity for $\eta_2 = 0.1$ or $\eta_2 = 0$, but $\eta_1 = 0.5$ gives an almost vanishing sensitivity. In principle, the results for η_2 can also be transferred to η_3. A special characteristic is a high sensitivity for $\eta_3 = 0.1$ near to the end of the epidemic. Figure 13 shows how the number of deaths depends on η_1. A small η_1 gives also a small overall death toll. Changes of β or γ may alter this behaviour significantly in accordance to our stability analysis results.

6.6 Observation Correctness ε

The sensitivity of the system concerning observation correctness ε is depicted in Figure 11. The three values $\varepsilon = 0.4$ (brown), $\varepsilon = 0.6$ (pink) and especially $\varepsilon = 1.0$ (blue) stand out. The entirety of possible behaviors of the system is probably the richest for these three values. Other values of ε become dominant, though, when the values of the system parameters are changed. As an example, consider the effects of a decrease of p_c from 0.75 to 0.4 in Figure 12.

The effects of an observational error ε on the course of an epidemic are shown in Figure 14. The overall system does not react sensitively on changes of the parameters α, δ, σ, λ, p_a or p_c. Conversely, a variation of the parameters p_f, γ or β may alter the evolution significantly.

7 Limitations of Model and Analysis

Several simplifications have been applied in order to make the epidemics model tractable. We neglect, for example, the existence of concurrent virus strains or the heterogeneity of the population. Only a rudimentary set of frictions is taken into account. In this respect the consequences of various frictions will be of interest. The paper intents to discuss some basic ideas on how to deal with frictions rather than to perform an analysis of the effects of specific frictions, though.

The analysis of the control unit function deserves more attention. The same holds for deriving control strategies from the properties of the underlying epidemics model. A candidate approach for deriving such strategies would be evolutionary optimization.

Variants of the score function and of the rule system will eventually modify the results. One may ask, which version is preferable from the viewpoint of controllability and robustness. It is reasonable that in different regions of the parameter space, different rule systems may have to be preferred. The investigation of potential phase transitions of systems behavior may also to be subject of future research.

8 Discussion and Outlook

The paper investigates strategies of epidemics management in presence of frictions. The inclusion of frictions seems to be mandatory for discussing the behavior of a *realistic* control component, because the preferable mix of countermeasures may depend on the scale of the frictions. Furthermore, different countermeasures may be affected by different frictions in a

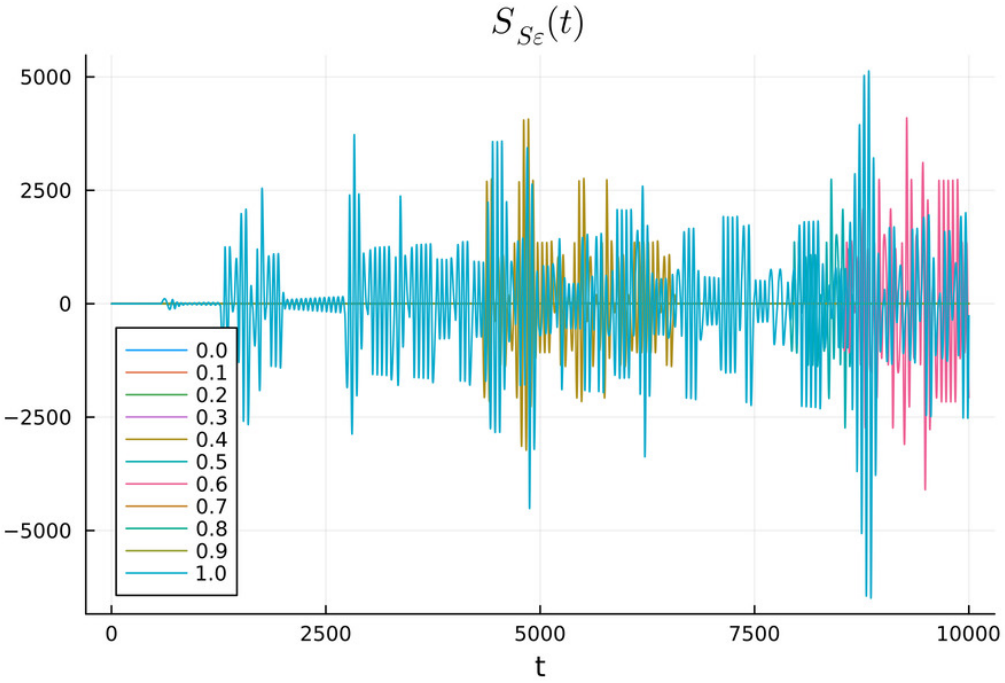

Figure 11: Sensitivity function $S_{S\varepsilon}$. The behaviour of $S_{E\varepsilon}$, $S_{I\varepsilon}$, $S_{H\varepsilon}$, $S_{C\varepsilon}$, $S_{R\varepsilon}$, $S_{D\varepsilon}$ is quite similar to that of $S_{S\varepsilon}$.

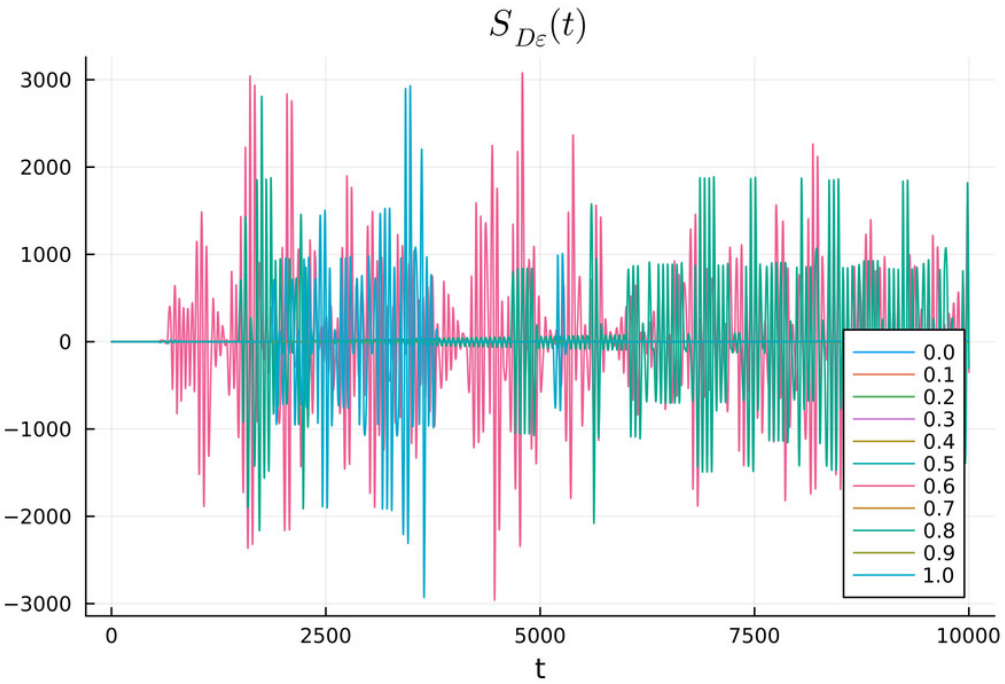

Figure 12: $S_{D\varepsilon}$ for $p_c = 0.4$

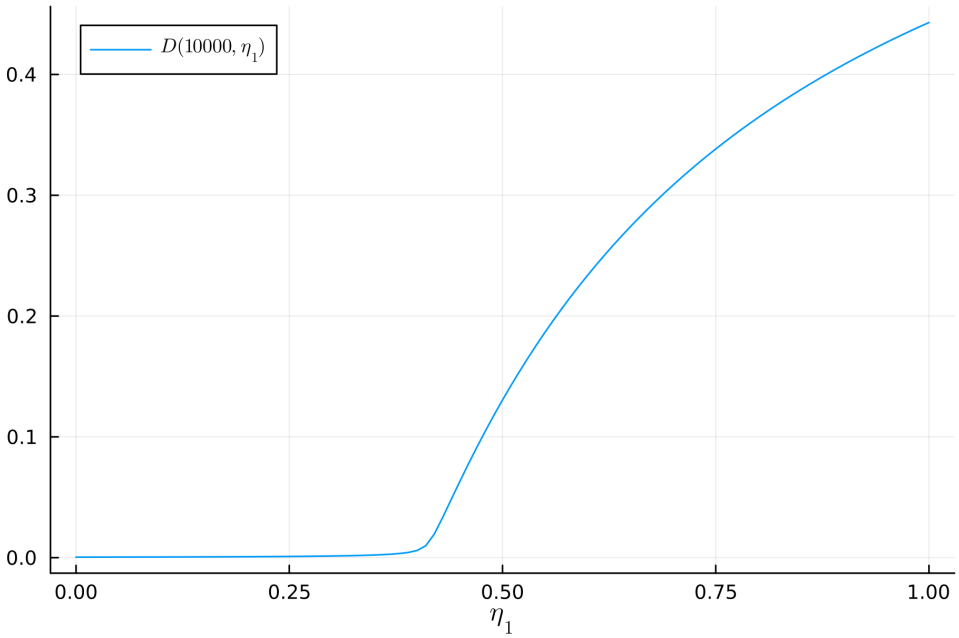

$\alpha = 0.3$	$\gamma = 0.01$	$\sigma = 0.5$	$p_a = 0.79$	$p_f = 0.33$	$\nu = 0.01$
$\beta = 0.05$	$\delta = 0.15$	$\lambda = 0.5$	$p_c = 0.12$		$\mu = 0.01$

Figure 13: Number D of cummulative deaths after 10000 time steps in dependence of the parameter η_1

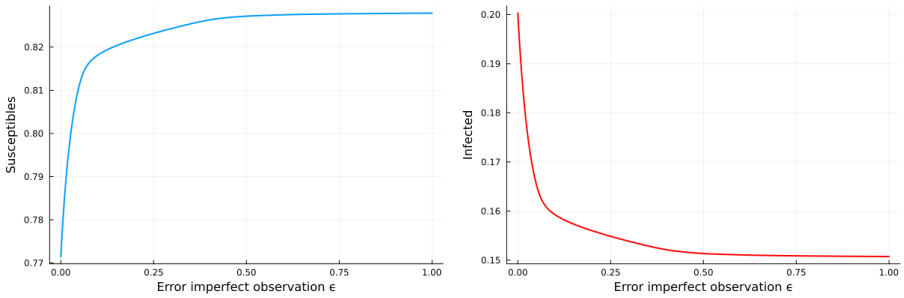

$\alpha = 0.3$	$\gamma = 0.01$	$\sigma = 0.5$	$p_a = 0.12$	$p_f = 0.33$	$\nu = 0.01$
$\beta = 0.05$	$\delta = 0.15$	$\lambda = 0.5$	$p_c = 0.79$		$\mu = 0.01$
$\eta = 0.5$					

Figure 14: Correlation susceptibles-error and infected-error respectively.

different way. To be useful for predictive purposes, however, a much broader range of frictions needs to be analyzed than here.

The model may be extended such that multi-domain aspects are taken into account. Countermeasures, which are useful for containing epidemics, may at least partially counteracting economic welfare, individual freedom, psychological welfare and so on [4, 8]. Accordingly, countermeasures are not effective from the beginning in our model but triggered depending on the current situation. The paper focuses on COVID-19; the state of affairs in case of other diseases is an open question. The discussion of the influence of additional details like the interplay between a control unit and a population with only partial compliance to the regulations raised by the control unit would be of interest as well. A disadvantageous outcome of an outbreak may not only be caused by inappropriate countermeasures, but also by the unwillingness of the population to follow suitable countermeasures.

Based on the considerations in the paper, it may be feasible to refine the organizational processes that serve as primary bottleneck in intervention management. Furthermore, decision-makers tasked with choosing appropriate countermeasures may perhaps be able to enhance the quality of their predictions. Last but not least, our considerations are not only applicable to epidemic contexts. The fundamental approach outlined here is adaptable to various other crisis management scenarios as well.

References

[1] Event handling and callback functions · differentialequations.jl. https://docs.sciml.ai/DiffEqDocs/stable/features/callback_functions/.

[2] Meoni. https://www.ars.toscana.it/2-articoli/4581-nuovo-sistema-a-colori-per-monitoraggio-pandemia-nuovo-coronavirus-cambiano-criteri-classificazione-fasce-di-rischio.html.

[3] Pandemieradar. https://www.rki.de/DE/Content/InfAZ/N/Neuartiges_Coronavirus/Situationsberichte/COVID-19-Trends/COVID-19-Trends.html?__blob=publicationFile#/home.

[4] P. Antras, S. J. Redding, and E. A. Rossi-Hansberg. Globalization and pandemics. *NBER Working Paper No. w27840*, 2020.

[5] J. Bezanson, A. Edelman, S. Karpinski, and V. B. Shah. Julia: A fresh approach to numerical computing. *SIAM Review*, 59(1):65–98, 2017.

[6] A. W. Byrne, D. McEvoy, A. B. Collins, K. Hunt, M. Casey, A. Barber, F. Butler, J. Griffin, E. A. Lane, C. McAloon, et al. Inferred duration of infectious period of SARS-CoV-2: rapid scoping review and analysis of available evidence for asymptomatic and symptomatic COVID-19 cases. *BMJ open*, 10(8):e039856, 2020.

[7] L. Cuesta Herrera, L. Pastenes, F. Córdova-Lepe, A. Arencibia, H. Torres-Mantilla, and J. Gutiérrez-Jara. Analysis of SEIR-type models used at the beginning of COVID-19 pandemic reported in high-impact journals. *Medwave*, 22:e2552–e2552, 09 2022.

[8] T. Daghriri and O. Ozmen. Quantifying the effects of social distancing on the spread of COVID-19. *International Journal of Environmental Research and Public Health*, 18(11), 2021.

[9] C. Dai, J. Yang, and K. Wang. Evaluation of prevention and control interventions and its impact on the epidemic of coronavirus disease 2019 in Chongqing and Guizhou provinces. *Mathematical Biosciences and Engineering*, 17(4):2781–2791, 2020.

[10] J. Draeger. Roadmap to a unified treatment of safety and security. In *Proceedings of the 10th Conference on System Safety and Cyber Security*. IET, 2015.

[11] J. Draeger. Safety, security, and social engineering - thoughts, challenges and a concept of quantitative risk assessment. In J. M. Holder, editor, *A closer look at safety and security*, chapter 3. Nova Science Publishers, Inc., 2020.

[12] J. Draeger and S. Hahndel. Formalized risk assessment for safety and security. *preprint arXiv:1709.00567v2*, 2017.

[13] E. Fernández-Carrión, B. Ivorra, B. Martínez-López, A. Ramos, and J. Sánchez-Vizcaíno. Implementation and validation of an economic module in the Be-FAST model to predict costs generated by livestock disease epidemics: Application to classical swine fever epidemics in Spain. *Preventive Veterinary Medicine*, 126:66–73, 2016.

[14] T. Fischer, T. Gerwald, S. Lajos, S. Woellert, C. Kuttler, and J. Draeger. A model of the mutual influence between epidemics and rumors using Covid-19 as an example. Technical report, Technical University of Munich and IABG mbH, 2022.

[15] T. Fischer, T. Gerwald, S. Lajos, S. Woellert, C. Kuttler, and J. Draeger. Modeling the influence of the information domain on countermeasure effectiveness in case of COVID-19. In *Journal of Physics: Conference Series*, volume 2514, page 012009. IOP Publishing, 2023.

[16] B. Gates. The next outbreak? We're not ready, 2015. TED Talk.

[17] B. Gates. *How to prevent the next pandemic*. Vintage, 2022.

[18] R. Greifeneder, M. Jaffe, E. Newman, and N. Schwarz. *The psychology of fake news: Accepting, sharing, and correcting misinformation*. Routledge, 2021.

[19] L. Hawryluck, W. L. Gold, S. Robinson, S. Pogorski, S. Galea, and R. Styra. SARS control and psychological effects of quarantine, Toronto, Canada. *Emerging infectious diseases*, 10(7):1206, 2004.

[20] C. Kamp. Demographic and behavioural change during epidemics. *Procedia Computer Science*, 1(1):2253–2259, 2010. ICCS 2010.

[21] M. E. Kretzschmar, B. Ashby, E. Fearon, C. E. Overton, J. Panovska-Griffiths, L. Pellis, M. Quaife, G. Rozhnova, F. Scarabel, H. B. Stage, B. Swallow, R. N. Thompson, M. J. Tildesley, and D. Villela. Challenges for modelling interventions for future pandemics. *Epidemics*, 38:100546, 2022.

[22] R. C. Larson and K. R. Nigmatulina. Engineering responses to pandemics. *Information Knowledge Systems Management*, 8(1-4):311–339, 2009.

[23] S. A. Lauer, K. H. Grantz, Q. Bi, F. K. Jones, Q. Zheng, H. R. Meredith, A. S. Azman, N. G. Reich, and J. Lessler. The incubation period of coronavirus disease 2019 (covid-19) from publicly reported confirmed cases: estimation and application. *Annals of internal medicine*, 172(9):577–582, 2020.

[24] R. J. LeClaire, D. Pasqualini, A. Bandlow, M. Ewers, J. M. Fair, and G. B. Hirsch. A prototype desktop simulator for infrastructure protection: an application to decision support for controlling infectious disease outbreaks. In *International Conference of the System Dynamics Society, Boston, Ma*, 2007.

[25] E. K. Lee, Y. Liu, F. Yuan, and F. H. Pietz. Strategies for disease containment: A biological-behavioral-intervention computational informatics framework. In *AMIA Annual Symposium Proceedings*, volume 2021, page 687. American Medical Informatics Association, 2021.

[26] P. Loganathan. *Process Systems Engineering Approaches for Intervention Planning during Infectious Disease Outbreaks*. PhD thesis, University of Singapore, 2012.

[27] M. Martcheva. *An Introduction to Mathematical Epidemiology*. Springer US, Boston, MA, 2015.

[28] E. Mathieu, H. Ritchie, L. Rodés-Guirao, C. Appel, C. Giattino, J. Hasell, B. Macdonald, S. Dattani, D. Beltekian, E. Ortiz-Ospina, and M. Roser. Coronavirus pandemic (covid-19). *Our World in Data*, 2020. https://ourworldindata.org/coronavirus.

[29] C. McGowan, F. Cecere, R. Darneille, and N. Laverdure. Biological event modeling for response planning. In *Unifying Themes in Complex Systems: Proceedings of the Sixth International Conference on Complex Systems*, pages 374–381. Springer, 2010.

[30] M. Moslonka-Lefebvre, H. Monod, C. A. Gilligan, E. Vergu, and J. A. Filipe. Epidemics in markets with trade friction and imperfect transactions. *Journal of Theoretical Biology*, 374:165–178, 2015.

[31] C. Rackauckas and Q. Nie. Differentialequations.jl–a performant and feature-rich ecosystem for solving differential equations in julia. *Journal of Open Research Software*, 5(1):15, 2017.

[32] R. Richard, J. Casas, and E. McCauley. Sensitivity analysis of continuous-time models for ecological and evolutionary theories. *Theoretical Ecology*, 8(4):481–490, 2015.

[33] H. Ritchie, E. Mathieu, L. Rodés-Guirao, C. Appel, C. Giattino, E. Ortiz-Ospina, J. Hasell, B. Macdonald, D. Beltekian, and M. Roser. Coronavirus pandemic (covid-19). *Our world in data*, 2023.

[34] W. Shang, L. Kang, G. Cao, Y. Wang, P. Gao, J. Liu, and M. Liu. Percentage of asymptomatic infections among SARS-CoV-2 Omicron variant-positive individuals: A systematic review and meta-analysis. *Vaccines*, 10(7), 2022.

[35] P. Strong. Epidemic psychology: a model. *Sociology of Health & Illness*, 12(3):249–259, 1990.

[36] Y. Su, L. Pan, H. Yan, G. Zhang, and R. Zhang. Social simulation model of the spread and prevention of the omicron SARS-CoV-2 variant. *Axioms*, 11(12):660, 2022.

[37] C. Sy, E. Bernardo, A. Miguel, J. L. San Juan, A. P. Mayol, P. M. Ching, A. Culaba, A. Ubando, and J. E. Mutuc. Policy development for pandemic response using system dynamics: a case study on covid-19. *Process Integration and Optimization for Sustainability*, 4:497–501, 2020.

[38] C. Sy, P. M. Ching, J. L. San Juan, E. Bernardo, A. Miguel, A. P. Mayol, A. Culaba, A. Ubando, and J. E. Mutuc. Systems dynamics modeling of pandemic influenza for strategic policy development: a simulation-based analysis of the COVID-19 case. *Process Integration and Optimization for Sustainability*, pages 1–14, 2021.

[39] E. Unlu, H. Léger, O. Motornyi, A. Rukubayihunga, T. Ishacian, and M. Chouiten. Epidemic analysis of COVID-19 outbreak and counter-measures in france. 2020.

[40] V. Vasiliauskaite, N. Antulov-Fantulin, and D. Helbing. On some fundamental challenges in monitoring epidemics. *Phil. Trans. R. Soc. A.*, page 3802021011720210117, 2022.

[41] T. M. Wassenaar, V. Wanchai, G. Buzard, and D. W. Ussery. The first three waves of the Covid-19 pandemic hint at a limited genetic repertoire for SARS-CoV-2. *FEMS Microbiology Reviews*, 46(3):fuac003, 01 2022.

[42] H. Yang, S. Zhang, R. Liu, A. Krall, Y. Wang, M. Ventura, and C. Deflitch. Epidemic informatics and control: A holistic approach from system informatics to epidemic response and risk management in public health. In *AI and Analytics for Public Health-Proceedings of the 2020 INFORMS International Conference on Service Science*, pages 1–46. Springer Berlin/Heidelberg, Germany, 2021.

[43] F. Zurek, L. Schwarzmeier, B. Dionisi Ferrera, C. Kuttler, and J. Draeger. Managing epidemics: Dynamic countermeasures and frictions. 2024.